Article

Competing C#F Activation Pathways in the Reaction of Pt(0) with Fluoropyridines: Phosphine-Assistance versus Oxidative Addition

Ainara Nova, Stefan Erhardt, Naseralla A. Jasim, Robin N. Perutz, Stuart A. Macgregor, John E. McGrady, and Adrian C. Whitwood

J. Am. Chem. Soc., **2008**, 130 (46), 15499-15511 • DOI: 10.1021/ja8046238 • Publication Date (Web): 25 October 2008

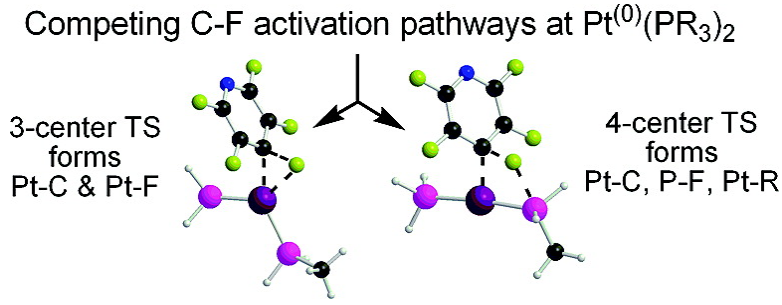

More About This Article

Additional resources and features associated with this article are available within the HTML version:

- Supporting Information
- Links to the 1 articles that cite this article, as of the time of this article download
- Access to high resolution figures
- Links to articles and content related to this article
- Copyright permission to reproduce figures and/or text from this article

View the Full Text HTML

J|A|C|S
ARTICLES

Published on Web 10/25/2008

Competing C−F Activation Pathways in the Reaction of Pt(0) with Fluoropyridines: Phosphine-Assistance versus Oxidative Addition

Ainara Nova,[†] Stefan Erhardt,[‡,⊥] Naseralla A. Jasim,[†] Robin N. Perutz,*[,†] Stuart A. Macgregor,*[,‡] John E. McGrady,*[,§] and Adrian C. Whitwood[†]

Department of Chemistry, University of York, Heslington, York YO10 5DD, United Kingdom, School of Engineering and Physical Sciences, Heriot-Watt University, Edinburgh EH14 4AS, United Kingdom, and WestCHEM, Department of Chemistry, University of Glasgow, Glasgow G12 8QQ, United Kingdom

Received June 24, 2008; E-mail: S.A.Macgregor@hw.ac.uk; j.mcgrady@chem.gla.ac.uk; rnp1@york.ac.uk

Abstract: A survey of computed mechanisms for C−F bond activation at the 4-position of pentafluoropyridine by the model zero-valent *bis*-phosphine complex, [Pt(PH$_3$)(PH$_2$Me)], reveals three quite distinct pathways leading to square-planar Pt(II) products. Direct oxidative addition leads to *cis*-[Pt(F)(4-C$_5$NF$_4$)(PH$_3$)(PH$_2$Me)] via a conventional 3-center transition state. This process competes with two different phosphine-assisted mechanisms in which C−F activation involves fluorine transfer to a phosphorus center via novel 4-center transition states. The more accessible of the two phosphine-assisted processes involves concerted transfer of an alkyl group from phosphorus to the metal to give a platinum(alkyl)(fluorophosphine), *trans*-[Pt(Me)(4-C$_5$NF$_4$)(PH$_3$)(PH$_2$F)], analogues of which have been observed experimentally. The second phosphine-assisted pathway sees fluorine transfer to one of the phosphine ligands with formation of a metastable metallophosphorane intermediate from which either alkyl or fluorine transfer to the metal is possible. Both Pt−fluoride and Pt(alkyl)(fluorophosphine) products are therefore accessible via this route. Our calculations highlight the central role of metallophosphorane species, either as intermediates or transition states, in aromatic C−F bond activation. In addition, the similar computed barriers for all three processes suggest that Pt−fluoride species should be accessible. This is confirmed experimentally by the reaction of [Pt(PR$_3$)$_2$] species (R = isopropyl (*i*Pr), cyclohexyl (Cy), and cyclopentyl (Cyp)) with 2,3,5-trifluoro-4-(trifluoromethyl)pyridine to give *cis*-[Pt(F){2-C$_5$NHF$_2$(CF$_3$)}(PR$_3$)$_2$]. These species subsequently convert to the *trans*-isomers, either thermally or photochemically. The crystal structure of *cis*-[Pt(F){2-C$_5$NHF$_2$(CF$_3$)}(P*i*Pr$_3$)$_2$] shows planar coordination at Pt with *r*(F−Pt) = 2.029(3) Å and P(1)−Pt−P(2) = 109.10(3)°. The crystal structure of *trans*-[Pt(F){2-C$_5$NHF$_2$(CF$_3$)}(PCyp$_3$)$_2$] shows standard square-planar coordination at Pt with *r*(F−Pt) = 2.040(19) Å.

1. Introduction

The group 10 metals have played a key role in the development of the C−F bond activation chemistry of fluoroaromatics and fluoroheteroaromatics.[1,2] Intermolecular C−F oxidative addition of hexafluorobenzene has been observed at a number of nickel species, including [Ni(*t*Bu$_2$PCH$_2$CH$_2$P*t*Bu$_2$)],[3] [Ni(PEt$_3$)$_2$],[4] and [Ni(*i*Pr$_2$Im)$_2$] (*i*Pr$_2$Im = 1,3-di(isopropyl)imidazol-2-ylidene).[5] The corresponding reactions of fluorinated pyridines and pyrimidines at [Ni(PEt$_3$)$_2$] proceed even more readily, and an extensive chemistry based on these reactions has been developed, providing routes to a number of hitherto inaccessible selectively fluorinated species.[1b,4,6] Comparable reactions of fluorinated pyridines and pyrimidines have also been reported with [Pd(PR$_3$)$_2$] complexes, although the regioselectivity of attack is somewhat different from the corresponding

[†] University of York.
[‡] Heriot-Watt University.
[§] University of Glasgow.
[⊥] Present Address: Max-Planck-Institut für Kohlenforschung, Kaiser-Wilhelm-Platz 1, 45470 Mülheim an der Ruhr, Germany.

(1) (a) Braun, T.; Perutz, R. N. Transition-Metal Mediated C-F Bond Activation. In *Comprehensive Organometallic Chemistry III*; Crabtree, R. H.; Mingos, D. M. P.; Elsevier: Amsterdam, 2006; Vol. 1, Chapter 26. (b) Braun, T.; Perutz, R. N. *Chem. Commun.* **2002**, 2749.
(2) (a) Torrens, H. *Coord. Chem. Rev.* **2005**, *249*, 1957. (b) Burdeniuc, J.; Jedlicka, B.; Crabtree, R. H. *Chem. Ber.* **1997**, *130*, 145. (c) Murphy, E. F.; Murugavel, R.; Roesky, H. W. *Chem. Rev.* **1997**, *97*, 3425. (d) Kiplinger, J. L.; Richmond, T. G.; Osterberg, C. E. *Chem. Rev.* **1994**, *94*, 373. (e) Jones, W. D. *Dalton Trans.* **2003**, 3991.
(3) Bach, I.; Pörschke, K.-R.; Goddard, R.; Kopiske, C.; Krüger, C.; Rufinska, A.; Seevogel, K. *Organometallics* **1996**, *15*, 4959.
(4) (a) Cronin, L.; Higgitt, C. L.; Karch, R.; Perutz, R. N. *Organometallics* **1997**, *16*, 4920. (b) Archibald, S. J.; Braun, T.; Gaunt, J. F.; Hobson, J. E.; Perutz, R. N. *J. Chem. Soc., Dalton Trans.*, **2000**, 2013. (c) Braun, T.; Cronin, L.; Higgitt, C. L.; McGrady, J. E.; Perutz, R. N.; Reinhold, M. *New J. Chem.* **2001**, *25*, 19. (d) Burling, S.; Elliott, P. I. P.; Jasim, N. A.; Lindup, R. J.; McKenna, J.; Perutz, R. N.; Archibald, S. J.; Whitwood, A. C. *Dalton Trans.* **2005**, 3686.
(5) (a) Schaub, T.; Radius, U. *Chem. Eur. J.* **2005**, *11*, 5024–5030. (b) Schaub, T.; Backes, M.; Radius, U. *J. Am. Chem. Soc.* **2006**, *128*, 15964.
(6) (a) Braun, T.; Foxon, S. P.; Perutz, R. N.; Walton, P. H. *Angew. Chem., Int. Ed.* **1999**, *38*, 3326. (b) Steffen, A.; Sladek, M. I.; Braun, T.; Neumann, B.; Stammler, H.-G. *Organometallics* **2005**, *24*, 4057.

Scheme 1

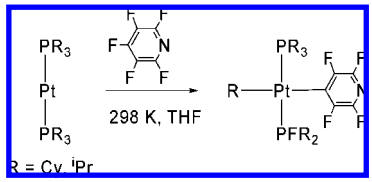

reactions at nickel.[7,8] The facile oxidative addition of C−F bonds at both nickel and palladium has recently been exploited in catalytic cross-coupling reactions.[9] A more comprehensive introduction to C−F activation is given in the previous paper in this issue.[10]

In contrast to the classic C−F intermolecular oxidative addition chemistry accessible to nickel and palladium, such reactions have been almost completely absent from platinum chemistry (but intramolecular reactions are more common).[11] Prior to the present work only a single example of Pt−fluoride formation by intermolecular reaction has been reported via the reaction of [Pt(*t*Bu$_2$PCH$_2$P*t*Bu$_2$)] with C_6F_6.[12] Instead, the reaction of [Pt(PR$_3$)$_2$] species (R = Cy, *i*Pr) with pentafluoropyridine yields a completely different outcome, in which a fluorine atom migrates to one of the phosphine ligands, displacing an alkyl substituent, R, which is transferred to Pt (Scheme 1).[7] The net result is a Pt(alkyl)(fluorophosphine), *trans*-[Pt(R)(4-C_5NF_4)(PR$_3$)(PR$_2$F)], and not the Pt−fluoride anticipated from conventional oxidative addition. Grushin et al. have shown that analogous Pt−alkyl products are obtained in the reaction of [Pt(PR$_3$)$_2$] with hexafluorobenzene.[13] The fact that oxidative addition of a C−F bond at platinum has only been observed with the highly constrained [Pt(*t*Bu$_2$PCH$_2$P*t*Bu$_2$)] system with a small bite-angle chelating phosphine makes it tempting to speculate that formation of Pt(alkyl)(fluorophosphine) products is the "normal" outcome of the reaction of fluoroaromatics with *bis*-trialkylphosphine complexes of Pt(0).[14]

Previous computational papers on aromatic C−F activation at group 10 metal centers concerned the reaction of [Pd(PH$_3$)$_2$] with C_6H_5F and other monofluorinated aromatics: the barriers to concerted oxidative addition were found to be 40 kcal/mol, reducing to 28 kcal/mol with 4-nitro substitution.[15] The introduction of an ortho carboxylate group can also promote reaction.[16] McGrady and Perutz have also compared the reactivity of hexafluorobenzene with that of benzene at [M(H$_2$PCH$_2$CH$_2$PH$_2$)] and [M(PH$_3$)$_2$] (M = Ni, Pt).[17] C−F oxidative addition in these cases proceeds via a classic 3-centered transition state (**A**: see below) and is invariably exothermic.

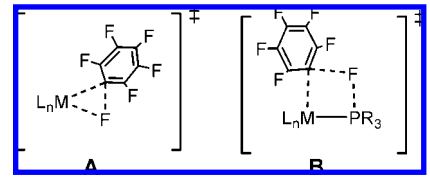

In the preceding paper in this issue,[10] Macgregor and Erhardt discussed the reaction of hexafluorobenzene with the electron-rich Ir(I) complex, [IrMe(PEt$_3$)$_3$], to form *trans*-[Ir(C_6F_5)-(PEt$_3$)$_2$(PEt$_2$F)].[18] There it was shown that the phosphine ligands can play an active role in a novel "phosphine-assisted" C−F activation process which involves a 4-centered transition state (**B**). In the present paper we build on these ideas in order to establish a clear understanding of aromatic C−F bond activation chemistry at platinum. In the computational section, we characterize pathways leading to Pt−alkyl and Pt−fluoride products which feature both 3-centered concerted oxidative addition and 4-centered phosphine-assisted transition states. These pathways are very finely balanced, suggesting that subtle changes to the system may induce a switch from one pathway to another. We then provide new experimental data in support of this proposal, and show that platinum complexes with simple monodentate phosphine ligands, [Pt(PR$_3$)$_2$], *can* be directed to form Pt−fluoride products with the highly electron-deficient fluoropyridine derivative, 2,3,5-trifluoro-4-(trifluoromethyl)pyridine, $C_5NHF_3(CF_3)$.

2. Results

2.1. Computational Studies on the Reactions of [Pt(PH$_3$)-(PH$_2$Me)] with Pentafluoropyridine. 1. Choice of Model System. In order to rationalize the formation of Pt(alkyl)(fluorophosphine) species, [Pt(R)(Ar^F)(PR$_3$)(PR$_2$F)], we have investigated the potential energy surface for the C−F activation reactions between pentafluoropyridine and the simple bis-phosphine model complex [Pt(PH$_3$)(PH$_2$Me)]. This choice of model system requires some comment. The experimental results involve a diverse range of phosphine ligands, PR$_3$, where R is any of *i*Pr, Cy or Cyp; the accurate modeling of such systems would represent a major challenge due to their conformational flex-

(7) Jasim, N. A.; Perutz, R. N.; Whitwood, A. C.; Braun, T.; Izundu, J.; Neumann, B.; Rothfeld, S.; Stammler, H. G. *Organometallics* **2004**, *23*, 6140.
(8) Braun, T.; Schorlemer, V.; Neumann, B.; Stammler, H.-G. *J. Fluorine Chem.* **2006**, *127*, 367.
(9) (a) Braun, T.; Perutz, R. N.; Sladek, M. I. *Chem. Commun.* **2001**, 2254. (b) Steffen, A.; Sladek, M. I.; Braun, T.; Neumann, B.; Stammler, H. G. *Organometallics* **2005**, *24*, 4057. (c) Kiso, Y.; Tamao, K.; Kumada, M. *J. Organomet. Chem.* **1973**, *50*, C12–C14. (d) Böhm, V. P. W.; Gstöttmayr, C. W. K.; Weskamp, T.; Herrmann, W. A. *Angew. Chem., Int. Ed.* **2001**, *40*, 3387. (e) Dankwardt, J. W. *J. Organomet. Chem.* **2005**, *690*, 932. (f) Ackermann, L.; Born, R.; Spatz, J. H.; Meyer, D. *Angew. Chem., Int. Ed.* **2005**, *44*, 7216. (g) Lamm, K.; Stollenz, M.; Meier, M.; Gorls, H.; Walther, D. *J. Organomet. Chem.* **2003**, *681*, 24. (h) Mongin, F.; Mojovic, L.; Guillamet, B.; Trecourt, F.; Queguiner, G. *J. Org. Chem.* **2002**, *67*, 8991. (i) Widdowson, D. A.; Wilhelm, R. *Chem. Commun.* **2003**, 578. (j) Widdowson, D. A.; Wilhelm, R. E. *Chem. Commun.* **1999**, 2211–2212. (k) Wilhelm, R.; Widdowson, D. A. *J. Chem. Soc., Perkin Trans. 1* **2000**, 3808.
(10) Erhardt, S.; Macgregor, S. A. *J. Am. Chem. Soc.* **2008**, *130*, 15490.
(11) Intramolecular oxidative addition of C−F bonds in Schiff base ligands bearing fluoroaromatic substituents has been observed in Pt(0) and Pt(II) complexes, and Pt-catalyzed cross coupling of such C−F bonds has also been observed. See: (a) Crespo, M.; Granell, J.; Font-Badia, M.; Solans, X. *J. Organomet. Chem.* **2004**, *689*, 3088. (b) Crespo, M.; Martines, M.; Sales, J. *Organometallics* **1993**, *12*, 4297. (c) Wang, T.; Alfonso, B. J.; Love, J. A. *Org. Lett.* **2007**, *9*, 5629.
(12) Hofmann, P.; Unfried, G. *Chem. Ber.* **1992**, *125*, 659.
(13) Macgregor, S. A.; Roe, D. C.; Marshall, W. J.; Bloch, K. M.; Bakhmutov, V. I.; Grushin, V. V. *J. Am. Chem. Soc.* **2005**, *127*, 15304.
(14) The use of a chelating *bis*-phosphine ligands would be expected to promote oxidative addition. See: (a) Kozuch, S.; Amatore, C.; Jutand, A.; Shaik, S. *Organometallics* **2005**, *24*, 2319. (b) Su, M.; Chu, S. *Inorg. Chem.* **1998**, *37*, 3400. (c) Sakaki, S.; Biswas, B.; Sugimoto, M. *J. Chem. Soc., Dalton Trans.* **1997**, 803.
(15) Jakt, M.; Johannissen, L.; Rzepa, H. S.; Widdowson, D. A.; Wilhelm, R. *J. Chem. Soc., Perkin Trans. 2,* **2002**, 576.
(16) Bahmanyar, S.; Borer, B. C.; Kim, Y. M.; Kurtz, D. M.; Yu, S. *Org. Lett.* **2005**, *7*, 1011.
(17) Reinhold, M.; McGrady, J. E.; Perutz, R. N. *J. Am. Chem. Soc.* **2004**, *126*, 5268.
(18) Blum, O.; Frolow, F.; Milstein, D. *J. Chem. Soc., Chem. Commun.* **1991**, 258.

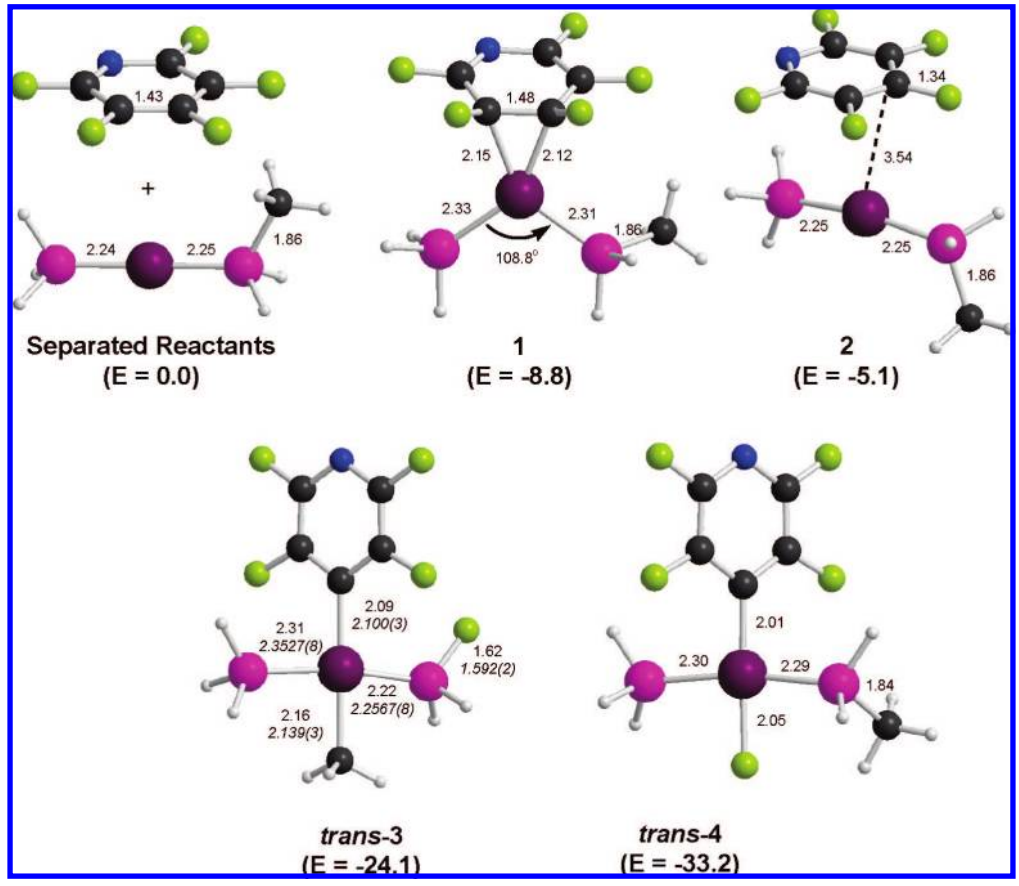

Figure 1. Computed structures of the separated reactants, precursor adducts (**1** and **2**), and alternative products ***trans*-3** and ***trans*-4** with distances in Å. For ***trans*-4** selected experimental data for *trans*-[Pt(Cy)(4-C_5NF_4)(PCy_3)(PCy_2F)][7] are shown in italics.

ibility. Instead, we have chosen to consider the *general* factors controlling C−F activation in [Pt(PR_3)$_2$]/C_5NF_5 systems. The experimental products require alkyl group transfer from phosphine to metal, and so we have retained one phosphine methyl group in order to model this appropriately.

2.2. Geometries of Complexes and Overall Reaction Energetics. As an initial step, we computed the overall energy change for the formation of the alternative Pt−fluoride and Pt(alkyl)(fluorophosphine) products. The reactant and product species concerned are shown in Figure 1, where all energies are quoted relative to those of the isolated reactants. Two distinct forms of the initial adduct between [Pt(PH_3)(PH_2Me)] and C_5NF_5 were located, the more stable of which is an η^2-arene complex (**1**, $E = -8.8$ kcal/mol). This exhibits an approximately trigonal-planar geometry with a P−Pt−P angle of 109° and significant elongation of the C3−C4 bond interacting with the Pt center (1.48 Å). A noncovalently bound species (**2**, $E = -5.1$ kcal/mol) was also found, in which the geometries of the two reactants are effectively unchanged from the isolated species. The computed energies indicate that **1** will be the dominant species available in solution.

The two putative Pt(II) products, *trans*-[Pt(Me)(4-C_5NF_4)(PH_3)(PH_2F)] (***trans*-3**) and *trans*-[Pt(F)(4-C_5NF_4)(PH_3)(PH_2Me)] (***trans*-4**), both show square-planar geometries, with ***trans*-3** exhibiting a longer Pt−fluoropyridyl distance (2.09 Å cf. 2.01 Å in ***trans*-4**) reflecting the much stronger trans influence of an alkyl compared to a fluoride ligand. The other significant difference is the short Pt−PFH_2 distance computed in ***trans*-3**, 2.22 Å, ∼0.08 Å shorter than the other Pt−P distances and indicative of a greater degree of π-back-donation to the fluorophosphine ligand. These trends are also seen in the experimental structure of *trans*-[Pt(Cy)(4-C_5NF_4)(PCy_3)(PCy_2F)], the key distances of which are included in italics in Figure 1.

The computed energies of ***trans*-3** and ***trans*-4** show that the formation of both species is favorable compared to that of the η^2-arene precursor, **1**. More significantly, the Pt−fluoride species, ***trans*-4**, is computed to be 9.1 kcal/mol more stable than Pt−alkyl ***trans*-3**, and this preference is retained even when the full systems including the Cy groups are considered.[19] This indicates that the experimental observation of *trans*-[Pt(Cy)(4-C_5NF_4)(PCy_3)(PCy_2F)][20] must be kinetic rather than thermodynamic in origin. In the following section we therefore assess the possible mechanisms of C−F activation and the barriers to reaction, and consider the competition between conventional oxidative addition and phosphine-assisted C−F activation.

(19) Further test calculations on the full systems, *trans*-[Pt(Cy)(4-C_5NF_4)(PCy_3)(PCy_2F)] (based on the experimentally determined structure) and *trans*-[Pt(F)(4-C_5NF_4)(PCy_3)$_2$] (based on the structure of its Pd analogue)[7] show the preference for the Pt−F species to be virtually unchanged. This key result was also insensitive to the choice of functional and the use of larger basis sets including the incorporation of diffuse functions on fluorine atoms.

(20) We have also considered the alternative regioisomeric products formed through the C−F activation at the 2- or 3-positions of pentafluoropyridine. For ***trans*-3** the relative energies (kcal/mol) follow the trend, 4-C_5NF_4 (−24.1) < 3-C_5NF_4 (−23.6) ≪ 2-C_5NF_4 (−12.1), while the same trend is computed for ***trans*-4**, 4-C_5NF_4 (−33.2) < 3-C_5NF_4 (−32.5) ≪ 2-C_5NF_4 (−22.9). This order is consistent with the formation of *trans*-[Pt(Cy)(4-C_5NF_4)(PCy_3)(PCy_2F)] as the favored product (see Experimental Section), although the computed difference in energy of the 4- and 3-isomers is small. See the Supporting Information for details.

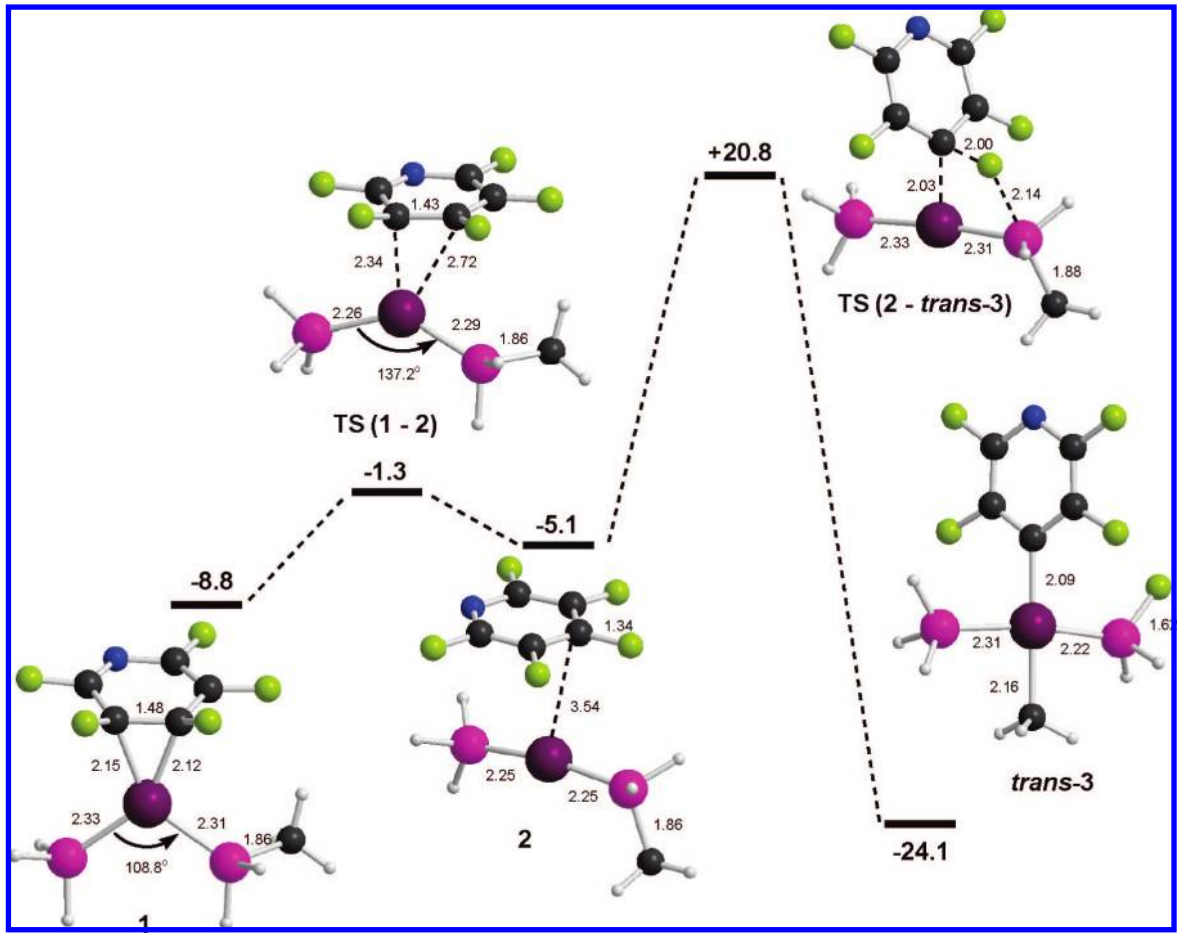

Figure 2. Computed energy profile (kcal/mol) for phosphine-assisted C−F activation via Pathway 1. Energies are relative to the isolated [Pt(PH_3)(PH_2Me)] and pentafluoropyridine reactants, and selected distances are given in Å.

2.3. Formation of Pt(Alkyl)(Fluorophosphine) Species. We have characterized two distinct phosphine-assisted reaction profiles, Pathways 1 and 2, for the C−F activation of pentafluoropyridine at the 4-position with [Pt(PH_3)(PH_2Me)] that are summarized in Figures 2 and 3, respectively. In both cases, the reaction must necessarily be initiated by the close approach of the pentafluoropyridine unit and the metal fragment to form either **1** or **2**. Along Pathway 1 the key C−F activation transition state was found to link to **2** and not **1**, and so the first step would therefore be dissociation of pentafluoropyridine from **1.** This can readily occur via a low-energy transition state, **TS(1−2)** ($E = -1.3$ kcal/mol), the barrier for this process being largely associated with the bending of the P−Pt−P angle.

From **2**, a C−F activation transition state, **TS(2-*trans*-3)** ($E = +20.8$ kcal/mol), was located in which the key C−F bond elongates to 2.00 Å, the F moves toward the PH_2Me group (P···F = 2.14 Å) and a very short Pt−C distance of 2.03 Å develops. Despite this, the Pt···F separation remains long (2.72 Å), and so **TS(2-*trans*-3)** corresponds to a 4-centered transition state in which the C−F bond effectively adds across the Pt−PH_2Me unit. At this point there is no significant movement of the methyl group toward the Pt center, and **TS(2-*trans*-3)** therefore resembles a metallophosphorane, featuring a formally anionic phosphoranide {PFH_2Me} moiety. Subsequent characterization of this transition state shows that it collapses directly to the Pt−(alkyl)(fluorophosphine) product, ***trans*-3**. Pathway 1 therefore involves a *concerted* activation of both the C−F and P−C bonds. The concerted nature of this process reflects the trans disposition of the {P−Pt−P} moiety, which maintains a near-linear arrangement throughout the reaction. As a consequence, the phosphoranide moiety develops cis to a vacant site, and thus the transfer of fluorine onto the PH_2Me ligand induces the concerted release of the methyl group onto Pt.

The alternative phosphine-assisted C−F activation process, Pathway 2, originates directly from the η^2-arene complex, **1** (see Figure 3). From **1**, a phosphine-assisted C−F activation transition state, **TS(1−5)**, was located with a computed relative energy of +24.5 kcal/mol. **TS(1−5)** is closely related to **TS(2-*trans*-3)**, with very similar distances within the 4-membered Pt−C−F−P ring (Pt−C = 2.01 Å C···F = 1.89 Å, P···F = 2.17 Å, Pt···F = 2.80 Å). However, in contrast to Pathway 1, the narrow P−Pt−P angle of only 110° in **TS(1−5)** means that the developing vacant site is now trans to the {PFH_2Me} moiety, and as a result the concerted transfer of the Me group to the metal center is blocked. Instead **TS(1−5)** links to a metallophosphorane intermediate, **5**, with an approximately T-shaped Pt(II) center. Complex **5** is marginally more stable than the separated reactants ($E = -2.0$ kcal/mol) and features a 5-coordinate trigonal-bipyramidal phosphorus center in which F and Me are in axial positions and the {Pt(PH_3)(Ar)} moiety is equatorial.

From metallophosphorane **5**, the formation of the final Pt(alkyl)(fluorophosphine) product, ***trans*-3**, can be effected by transfer of the Me group from the phosphoranide ligand to the Pt metal center. A transition state for this process was located (**TS(5-*trans*-3)**, $E = +8.3$ kcal/mol) in which rotation about

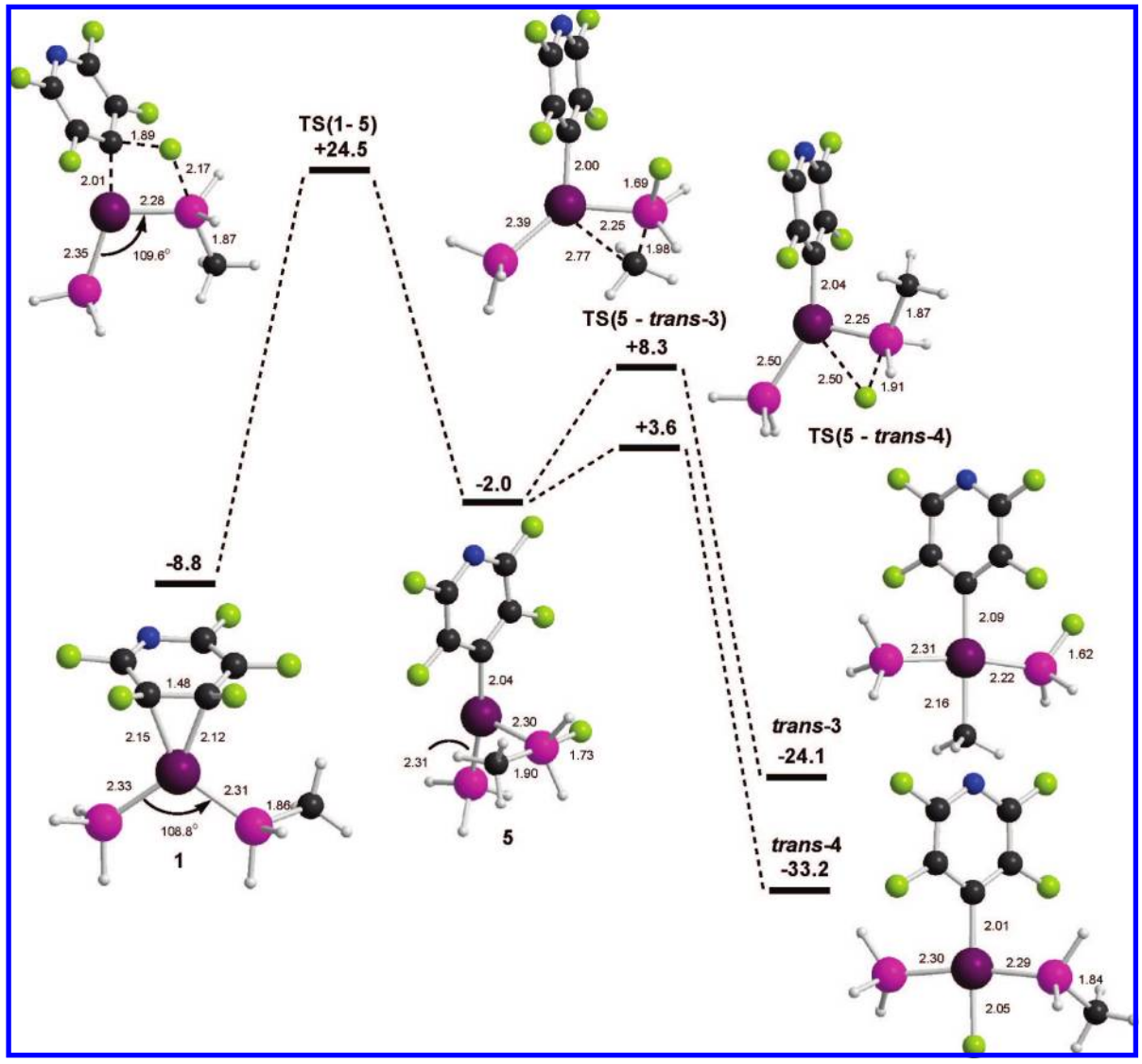

Figure 3. Computed energy profile (kcal/mol) for phosphine-assisted C−F activation via Pathway 2. From intermediate **5** Me transfer leads to ***trans*-3** (Pathway 2a), and F transfer yields ***trans*-4** (Pathway 2b). Energies are relative to the isolated [Pt(PH_3)(PH_2Me)] and pentafluoropyridine reactants, and selected distances are given in Å.

the Pt−PFH_2Me bond allows the Me group to approach the metal center (Pt···Me = 2.77 Å) while at the same time the P−Pt−P angle widens to 133° to accommodate the transferring Me group. Formation of ***trans*-3** via Pathway 2a is therefore a two-step process in which the initial phosphine-assisted C−F activation step via **TS(1−5)** is rate determining. Since **TS(1−5)** is 3.7 kcal/mol higher than **TS(2-*trans*-3)**, Pathway 1 should, on this basis, be the favored route for the formation of ***trans*-3**. The absolute barrier of 29.6 kcal/mol along Pathway 1 might be considered rather high, given that the experimental C−F activation reaction to give *trans*-[Pt(Cy)(4-C_5NF_4)(PCy_3)(PCy_2F)] is performed at room temperature. However, this reflects our choice of model system: with [Pt(PMe_3)$_2$] (which represents the electronic contribution of the trialkylphosphines more realistically) the barrier reduces to +24.8 kcal/mol. The reduced barrier with more electron-donating phosphine substituents is entirely consistent with our view of phosphine-assisted C−F activation in terms of a nucleophilic attack mechanism established in the preceding paper.[10,21]

2.4. Formation of Pt(Fluoride)(Phosphine) Species. In the preceding discussion we considered only methyl transfer from **5** to form ***trans*-3**. Metallophosphorane **5**, however, features both an axial Me and an axial F group on the 5-coordinate phosphorus center; thus, an analogous process involving F transfer leading to the Pt−fluoride species, ***trans*-4**, should also be possible (Pathway 2b), and a transition state for F transfer was indeed located (**TS(5-*trans*-4)**, E = +3.6 kcal/mol). As in **TS(5-*trans*-3)** the P−Pt−P angle widens (P−Pt−P = 112°) to create a vacant site at the metal, but in this case the rotation of the Pt−PFH_2Me bond is in the opposite sense such that the axial F approaches the metal center (Pt···F = 2.50 Å) and ultimately transfers to form ***trans*-4**. In fact, relative to the intermediate **5**, this F transfer process is much more accessible than methyl transfer via **TS(5-*trans*-3)**. However, it is important to recall the high energy of the preceding transition state **TS(1−5)** that means that both Pathways 2a and 2b are kinetically less accessible than Pathway 1, the concerted formation of ***trans*-3**. Nevertheless, the identification of species such as **5** as stable intermediates on the potential energy surface does suggest that

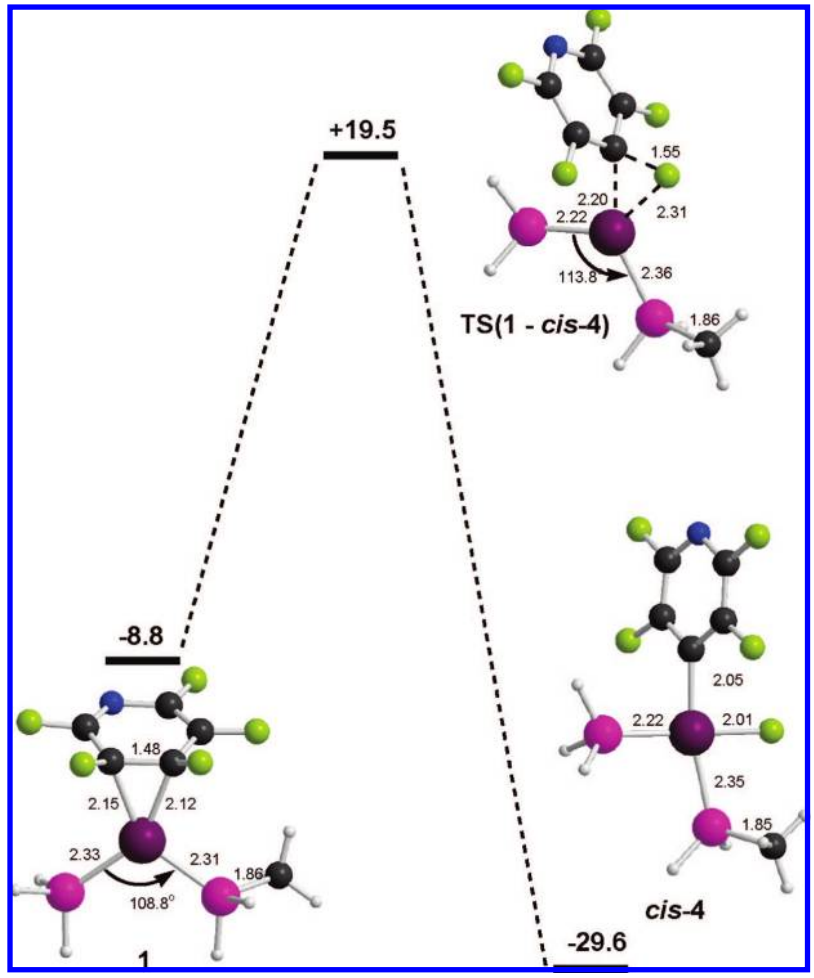

Figure 4. Computed energy profile for C−F oxidative addition along Pathway 3. Energies are given in kcal/mol relative to the isolated reactants, and selected distances are in Å.

novel phosphine-assisted routes to the formation of M−fluoride phosphine complexes may sometimes be accessible. Such a process could be considered a phosphine-assisted C−F oxidative addition.

Finally we consider the conventional route to M−fluoride complexes via concerted oxidative addition of a C−F bond. With [Pt(PH_3)(PH_2Me)] this would be expected to form *cis*-[Pt(C_5F_4N)(F)(PH_3)(PH_2Me)], ***cis*-4**, which could then undergo *cis/trans* isomerization to give ***trans*-4** (Pathway 3 in the following). Starting from the η^2-arene species **1** a 3-centered oxidative addition transition state, **TS(1-*cis*-4)**, was located at +19.5 kcal/mol, and product formation is strongly exothermic ($\Delta E = -20.8$ kcal/mol, see Figure 4). The single imaginary frequency at the transition state is associated with the C−F stretching mode, and the C−F bond is significantly elongated relative to those in free C_5F_5N (1.55 Å vs 1.35 Å). Moreover, the P−Pt−P angle of 114° accommodates the developing Pt−C and Pt−F bonds. This oxidative addition process is closely related, both structurally and energetically, to that computed for the activation of C_6F_6 discussed previously.[17] Several standard pathways could be conceived for subsequent *cis/trans* isomerization from ***cis*-5**. We shall not consider these here, although we shall return to the significance of the *cis/trans* isomerization below.

To summarize the computational results thus far, the calculations have revealed the presence of four quite distinct C−F activation pathways. Pathways 1 and 2a result in the formation of Pt−(alkyl)(fluorophosphine), ***trans*-3**, and of these two alternatives, Pathway 1, which involves a concerted phosphine-assisted process with a metallophosphorane transition state, lies lower. Pathways 2b and 3 yield Pt−fluoride complexes, ***trans*-4** for Pathway 2b and ***cis*-4** for Pathway 3. Of these channels, the concerted oxidative addition route, Pathway 3, is the more accessible. Thus, we conclude that the preference for fluoride or alkyl products in any given system will be determined by a competition between Pathways 1 and 3. Their barriers differ for our [Pt(PH_3)(PH_2Me)] model by only 1.3 kcal/mol.[22] In light of this small difference, it is reasonable to propose that subtle perturbations to the system, introduced through changing (i) the fluoroaromatic, (ii) the phosphine, or (iii) the conditions (solvent, temperature) may direct the reaction down different channels. In particular, although previously unobserved, conventional oxidative addition of a C−F bond at a Pt(0) *bis*-trialkylphosphine complex should be possible. In the next section, we report

(21) The barrier to phosphine-assisted C−F activation by [Pd(PH_3)(PH_2Me)] along Pathway 1 rises to +35.3 kcal/mol (relative to [Pd(PH_3)(PH_2Me)(η^2-C_5NF_5)]). This increased barrier is again consistent with a view of phosphine-assisted C−F activation proceeding via nucleophilic attack and this process being less accessible with the less electron-rich Pd center.

(22) Use of the [Pt(PMe_3)$_2$] model resulted in a reduction in the barrier along Pathway 3 to 24.8 kcal/mol. As essentially the same barrier was computed with this model along Pathway 1, this indicates that the key conclusion, i.e. that Pathways 1 and 3 are close in energy, is not affected by the choice of model.

Scheme 2

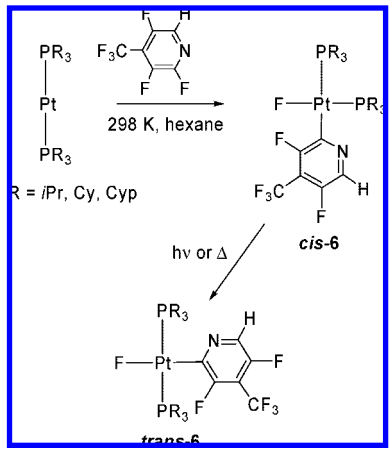

new experimental data showing that replacing pentafluoropyridine with 2,3,5-trifluoro-4-(trifluoromethyl)pyridine does just this, redirecting the reaction from platinum alkyl to platinum fluoride products.

2.5. Experimental Study of the Reaction of [Pt(PR$_3$)$_2$] with 2,3,5-Trifluoro-4-(trifluoromethyl)pyridine. A hexane solution (close to saturated) of freshly synthesized [Pt(P*i*Pr$_3$)$_2$] was treated with ∼2 equiv 2,3,5-trifluoro-4-(trifluoromethyl)pyridine, $C_5NHF_3(CF_3)$, at room temperature. The reaction mixture was left to react for 2 days in the glovebox, resulting in conversion to [Pt(F){2-$C_5NHF_2(CF_3)$}(P*i*Pr$_3$)$_2$], **6(*i*Pr)**, giving colorless crystals in yields up to 58%. The yield could be increased to 82% by leaving for a further week. The reaction was also conducted on an NMR scale in benzene-d_6 as solvent and monitored regularly by ^{19}F and ^{31}P NMR spectroscopy. Conversion to **6(*i*Pr)** was quantitative with no evidence for the formation of the alternative platinum(alkyl)(fluorophosphine) complex or any other platinum fluoride complexes. By far the dominant product was ***cis*-6(*i*Pr)** with only traces of ***trans*-6(*i*Pr)**. In the dark, ***cis*-6(*i*Pr)** proved to be stable for at least a month in solution at room temperature, but it is converted over the course of a few days to the *trans*-isomer by exposure to sunlight, or more rapidly by photolysis (see Scheme 2). *cis*/*trans* Isomerization can also be achieved by heating in benzene or THF (no decomposition is observed up to 70 °C).

The corresponding reactions with [Pt(PCy$_3$)$_2$] or [Pt(PCyp$_3$)$_2$] are slower, requiring up to 14 days (rate: Cyp > Cy), and yield colorless crystals of *trans*-[Pt(F){2-$C_5NHF_2(CF_3)$}(PCy$_3$)$_2$] ***trans*-6(Cy)**, and *trans*-[Pt(F)(2-$C_5NHF_2CF_3$)(PCyp$_3$)$_2$] ***trans*-6(Cyp)** in yields up to 83% and 69%, respectively. When the reactions were monitored daily as described above, a mixture of *cis* and *trans* products was observed in solution, the proportion of *trans* increasing with time. Once again, conversion to **6(Cyp)** and **6(Cy)** was quantitative with no evidence for the formation of the alternative platinum(alkyl)(fluorophosphine) complex or any other platinum fluoride complexes. These complexes are much more readily isolated than the hydride fluoride complex, *trans*-[Pt(H)(F)(PCy$_3$)$_2$], reported previously.[23]

2.6. NMR Spectra of 6. The ^{19}F NMR spectrum for 2,3,5-trifluoro-4-(trifluoromethyl)pyridine was analyzed for reference, and relevant data are listed in Table 1. The ^{19}F NMR spectrum of ***cis*-6(*i*Pr)** shows a doublet of doublets with platinum satellites at δ −253.4 (J_{PF} = 149.0 and 34.0, J_{PtF} = 330 Hz) (Figure 5a).

(23) Jasim, N. A.; Perutz, R. N. *J. Am. Chem. Soc.* **2000**, *122*, 8685.

The *trans*-isomer ***trans*-6(*i*Pr)** shows a triplet of doublets with platinum satellites at δ −314.5 (J_{PF} = 17.7, J_{FF} = 9.1, J_{PtF} = 251 Hz) (Figure 5b). These high-field resonances with large Pt−F coupling constants are characteristic of fluorine bonded to the platinum center. Complex ***cis*-6(*i*Pr)** also shows a triplet resonance at δ −57.8 (J_{FF} = 20.0 Hz) assigned to the CF_3 group of the aromatic ring with coupling to two fluorine nuclei ortho to the CF_3 group. A quartet resonance with platinum satellites δ −105.6 (J_{FF} = 21.0 Hz, J_{PtF} = 169 Hz) was assigned to the aromatic fluorine ortho to the platinum center, and a quartet resonance at δ −141.0 (J_{FF} = 21.0 Hz) assigned to the fluorine para to the platinum (Figure S2 (Supporting Information (SI)). (Note that coupling between the aromatic hydrogen and aromatic fluorine is negligible and there is no resonance in the region δ ∼−85 characteristic of fluorine ortho to nitrogen.) The resonances are consistent with the fluoropyridyl ring bonded to platinum at the 2-position. The fluoropyridyl resonances of ***trans*-6(*i*Pr)** are similar (Figure S5 (SI)).

The ^{31}P NMR spectrum of ***cis*-6(*i*Pr)** shows two resonances, a doublet of doublets with platinum satellites at δ 18.2 (J_{PF} =149.7, J_{PP} = 10, J_{PtP} = 4010 Hz) and a second doublet of doublets at δ 30.4 (J_{PP} = 9.9, J_{PF} = 33.9, J_{PtP} = 1852 Hz, see Figure S3 (SI)). The resonance with the larger P−F and P−Pt coupling constants is assigned to the phosphorus trans to the fluorine. The very low trans influence of fluorine results in an exceptionally large coupling constant for Pt(II).[24] The second resonance is assigned to the phosphorus trans to the fluoropyridyl group; its value of J_{PF} is small compared to the first due to the cis orientation of the fluorine. Its Pt−P coupling constant is also small compared to the first one due to the much larger trans influence of the fluoropyridyl group. The ^{31}P NMR spectrum of ***trans*-6(*i*Pr)** shows a doublet with platinum satellites at δ 33.5 (J_{PF} = 17.7, J_{PtP} = 2830 Hz, Figure S6 (SI)). The value of J_{PtP} is close to those of the *trans* platinum fluoride complexes, *trans*-[Pt(H)(FHF)(P*i*Pr$_3$)$_2$] J_{PtP} = 2860 Hz, J_{PF} = 9 Hz, and *trans*-[Pt(H)(F)(PCy$_3$)$_2$] J_{PtP} = 2938 Hz, J_{PF} = 11 Hz.[23]

The ^{1}H NMR spectrum for 2,3,5-trifluoro-4-(trifluoromethyl)-pyridine, run for reference, shows a broad singlet at δ 6.99. The ^{1}H NMR spectrum of ***cis*-6(*i*Pr)** shows a singlet at δ 8.32 assigned to the fluoropyridyl proton and a complicated multiplet at δ 1.37 assigned to the isopropyl CH_3 protons. Two multiplets at δ 2.23 and δ 2.57 simplify to two septets on ^{31}P decoupling, characteristic of the isopropyl CH protons (Figure S1 (SI)). The {^{1}H−^{31}P} correlation spectrum shows that the proton resonance at δ 2.23 couples to the ^{31}P resonance at δ 18.2, while the resonance at δ 2.57 couples to the ^{31}P resonance at δ 30.4. The ^{1}H NMR spectrum of ***trans*-6(*i*Pr)** shows two quartets for the methyl protons (δ 1.28 and 1.33) that simplify to doublets on ^{31}P decoupling (Figure S4 (SI)). There is a single multiplet for the CH protons that simplifies to a septet on ^{31}P decoupling. These patterns can be understood if there is restricted rotation about the Pt−P and P−C bonds that ensures that the two methyl groups of any isopropyl unit remain inequivalent.

The NMR data summarized in the previous paragraphs secure the assignments of ***cis*-6(*i*Pr)** and ***trans*-6(*i*Pr)** as *cis*- and *trans*-isomers of [Pt(F){2-$C_5NHF_2(CF_3)$}(P*i*Pr$_3$)$_2$]. These new experiments therefore demonstrate unambiguously that the platinum system can be switched from Pt−alkyl formation to Pt−fluoride

(24) (a) Yahav, A.; Goldberg, I.; Vigalok, A. *J. Am. Chem. Soc.* **2003**, *125*, 13634. (b) Yahav, A.; Goldberg, I.; Vigalok, A. *Inorg. Chem.* **2005**, *44*, 1547.

Table 1. NMR Data for $C_5NHF_3(CF_3)$ and Complexes ***cis*-6** and ***trans*-6** at 300 K in C_6D_6, δ (*J*/Hz)

product	^{1}H	^{19}F	^{31}P{H}
$C_5NHF_3CF_3$	6.99 (broad s)	−135.6 (m), F^4 −129.4 dqd (J_{FF} = 30, 19, 2.7), F^3 −85.9 (dd, J_{FF} = 30, 28 Hz), F^2 −57.9 (dd J_{FF} = 20.9 and 19.3), CF_3	
***cis*-6(*i*Pr)**	1.37, m (6H)	−253.4 (dd, 1F, J_{PF} = 149.0 and 34.0, J_{PtF} = 330), Pt−F	18.2 (dd, J_{PF} = 149.7, J_{PP} = 10.0, J_{PtP} = 4010 P trans to F
	2.23, m (1H) septet when ^{31}P decoupled, (J = 6.8)	−141.0 (q, 1F, J_{FF} = 21.0), F^5	30.4 dd (J_{PF} = 33.9, J_{PP} = 9.9, J_{PtP} = 1852), P trans to fluoropyridyl
	2.57 m (1H) septet when ^{31}P decoupled, (J = 6.8)	−105.6 (q, 1F, J_{FF} = 21.0, J_{PtF} =169), F^3	
	8.32 s (1H)	−57.8 (t, 3F, J_{FF} = 20.0), CF_3	
***trans*-6(*i*Pr)**	1.28 (q, 6H, J_{HH} = J_{HP} = 8), 1.33 (q, 6H, J_{HH} = J_{HP} = 8) (each is doublet when ^{31}P decoupled)[a]	−314.5 (td, 1F, J_{PF} = 17.7, J_{FF} = 9.1, J_{PtF} = 251), Pt−F	33.5 (d, J_{PF} =17.7, J_{PtP} = 2830)
	2.24 (2H) (J = 7)	−143.0 (q, 1F, J_{FF} = 18.0), F^5	
	8.39 s (1H)	−101.0 (qd, 1F, J_{FF} = 18.0 and 8.6, J_{PtF} = 292), F^3	
		−56.8 (t, 3F, J_{FF}= 18.0), CF_3	
***cis*-6(Cy)**	1.25−2.1 (m, 66H)	−252.9 (dd, 1F, J_{PF} = 150.0 and 32.0, J_{PtF} = 338), Pt−F	10.1 (dd, J_{PF} = 148.6, J_{PP} = 10.1, J_{PtP} = 4004), P trans to F
	8.52 (s, 1H)	−140.1 (q, 1F, J_{FF} = 23.0), F^5	21.0 (dd, J_{PF} = 32.5, J_{PP} = 10.2 J_{PtP} = 1834), P trans to fluoropyridyl
		−107.0 (q, 1F, J_{FF} = 20.0, J_{PtF} = 172), F^3	
		−56.6 (t, 3F, J_{FF} = 20.0), CF_3	
***trans*-6(Cy)**	1.0−2.5 (m, 66H)	−317.9 (t, 1F, J_{PF} =17.01 J_{PtF} = 227), Pt−F	25.5 (d J_{PF} =17.3, J_{PtP} = 2822)
	8.54 (s, 1H)	−144.2 (q, 1F, J_{FF} = 18.0), F^5	
		−101.1 (q, 1F, J_{FF} = 18.0, J_{PtF} = 299), F^3	
		−56.5 (t, 3F, (J_{FF} = 22.1), CF_3	
***cis*-6(Cyp)**	1.5−2.0 (m, 54H)	−261.3 (dd, 1F, J_{PF} = 154, J_{PF} = 36, J_{PtF} = 173), Pt−F	10.1 (dd, J_{PF} = 154, J_{PP} = 10.5, J_{PtP} = 4036), P trans to F
	8.50 (s, 1H)	−143.0 (q, 1F, J_{FF} = 23.0), F^5	20.4 (dd J_{PF} = 33.36, J_{PP} = 10.3 J_{PtP} = 1858), P trans to fluoropyridyl
		−108.3 (q, 1F, J_{FF} = 18.0, J_{PtF} = 181), F^3	
		−56.5 (t, 3F, J_{FF} = 20.0), CF_3	
***trans*-6(Cyp)**	0.5−2.0 (m, 54H)	−321.8 (t, 1F, J_{PF} = 17.4 J_{PtF} = 229), Pt−F	24.8 (d J_{PF} =17.5, J_{PtF} = 2828)
	8.44 (s, 1H)	−146 (q, 1F, J_{FF} = 19.0), F^5	
		−101.7 (q, 1F, J_{FF} = 18.0, J_{PtF} = 305), F^3	
		−60.1 (t, 3F, J_{FF} = 20.0), CF_3	

[a] Proved to arise from two separate resonances by comparing spectra at 500 and at 700 MHz.

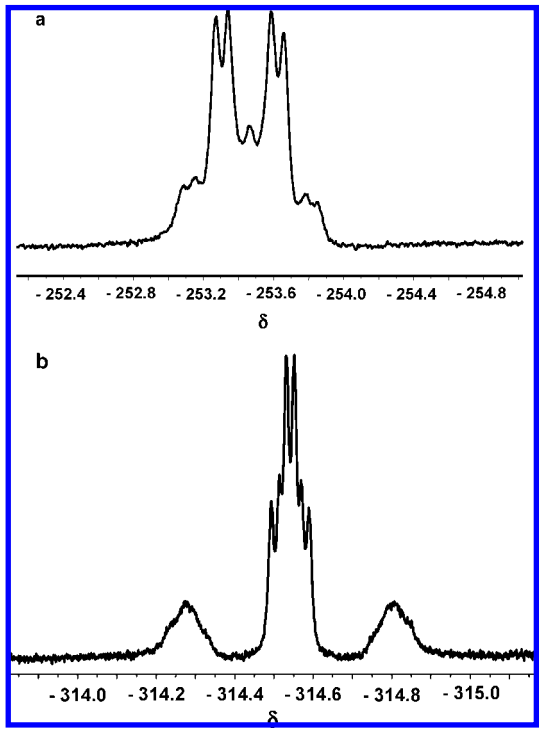

Figure 5. ^{19}F NMR spectra (470.4 MHz) in [$^2H_6$]benzene showing the Pt−F region of (a) ***cis*-6(*i*Pr)** and (b) ***trans*-6(*i*Pr)** (*cis*- and *trans*-[Pt(F){$C_5NHF_2(CF_3)$}($PiPr_3$)$_2$]).

formation with a small change of fluoropyridine. With the 4-position blocked by the highly electron-withdrawing CF_3 group, activation occurs at the 2-position and is also selective for the C−F over the C−H bond. The NMR spectra of ***cis*-6(Cy)** and ***cis*-6(Cyp)** are similar to those of ***cis*-6(*i*Pr)**, and those of ***trans*-6(Cy)** and ***trans*-6(Cyp)** are similar to those of ***trans*-6(*i*Pr)** (Table 1).

2.7. Crystal Structures of *cis*-6(*i*Pr) and *trans*-6(Cyp). Crystals of ***cis*-6(*i*Pr)** were obtained by slow crystallization of the reaction mixture in hexane solution and characterized by X-ray crystallography (Figure 6a, Table 2). The molecular structure shows a planar geometry at Pt with distortion from standard angles imposed by the cis disposition of the phosphine ligands (P(1)−Pt(1)−P(2) = 109.10(3)°, F(1)−Pt(1)−C(1) = 82.44(11)°, F(1)−Pt(1)−P(1) = 80.11(6)°). The Pt−C(fluoropyridyl) distance is 2.039(3) Å, while the Pt−F distance is 2.029(2) Å. As expected, the Pt−P distances are very different, 2.3884(8) Å for Pt−P(1) and 2.2258(9) Å for Pt−P(2), with the shorter distance for the phosphorus trans to fluorine. The difference of 0.163(1) Å reflects the very strong trans influence of the fluoropyridyl ligand and is fully consistent with the large difference between J_{PtPA} and J_{PtPB} (>2100 Hz). The CF_3 group exhibits rotational disorder and was refined with two different positions differing by a 60° rotation with occupancies of 85% and 15%. The maximum deviation from the best plane formed by C(1), F(1), P(1), P(2) is 0.080(2) Å, and the platinum atom lies 0.022 Å from this plane. The plane of the fluoropyridyl ring is rotated by 65.47(12)° relative to the best plane formed by C(1), F(1), P(1), and P(2). The nearest intermolecular contact to the fluoride bound to platinum is a hydrogen of a fluoropyridyl group at 2.44 Å.

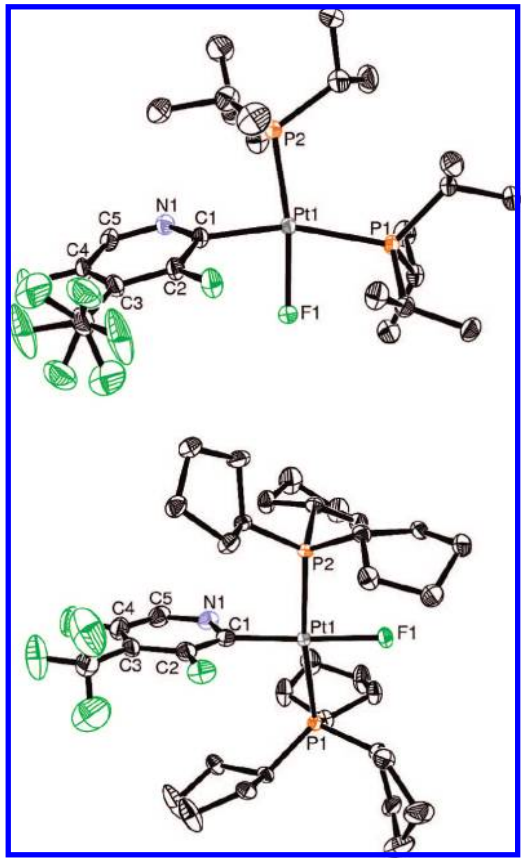

Figure 6. Molecular structures (50% ellipsoids, hydrogen atoms omitted) of ***cis*-6(*i*Pr)** (above) and ***trans*-6(Cyp)** (below).

Table 2. Selected bond lengths (Å) and angles (deg) of ***cis*-6(*i*Pr)** and ***trans*-6(Cyp)**

***cis*-6(*i*Pr)**		***trans*-6(Cyp)**		difference (***cis*-6(*i*Pr)** − ***trans*-6(Cyp))
bond	length (Å)	bond	length (Å)	length (Å)
C(1)−Pt(1)	2.039(3)	C(1)−Pt(1)	1.988(3)	+0.051(4)
F(1)−Pt(1)	2.029(2)	F(1)−Pt(1)	2.0402(19)	−0.011(3)
P(1)−Pt(1)	2.3884(8)	P(1)−Pt(1)	2.3224(8)	+0.066(1)
P(2)−Pt(1)	2.2258(9)	P(2)−Pt(1)	2.3225(7)	−0.097(1)
C(2)−F(2)	1.350(4)	C(2)−F(2)	1.366(4)	−0.016(6)

bond	angle (deg)	bond	angle (deg)
F(1)−Pt(1)−C(1)	82.44(11)	C(1)−Pt(1)−F(1)	174.27(12)
F(1)−Pt(1)−P(1)	80.11(6)	C(1)−Pt(1)−P(1)	95.69(9)
C(1)−Pt(1)−P(1)	161.78(10)	F(1)−Pt(1)−P(1)	84.51(6)
F(1)−Pt(1)−P(2)	170.55(6)	C(1)−Pt(1)−P(2)	92.11(9)
C(1)−Pt(1)−P(2)	88.57(10)	F(1)−Pt(1)−P(2)	87.42(6)
P(1)−Pt(1)−P(2)	109.10(3)	P(1)−Pt(1)−P(2)	171.62(3)

Colorless crystals of complex ***trans*-6(Cyp)** were obtained from a saturated hexane solution of the reaction mixture left in a glovebox at room temperature to crystallize overnight. The crystal structure was determined by X-ray diffraction at low temperature (Figure 6, Table 2). The molecular structure shows the expected trans disposition of the phosphine ligands with square-planar coordination at platinum. The Pt−C and Pt−F bond lengths are 1.988(3) and 2.0402(19) Å, respectively. The fluoropyridyl ring is rotated by 90.00(13)° relative to the C(1), P(2), P(2), F(1) best-fit plane. The nearest intermolecular contact to the fluoride bound to platinum is a hydrogen of a cyclopentyl group at 2.51 Å. We have also determined the crystal structure of ***trans*-6(Cy)**; details are described in the Supporting Information (Figures S7, S8 and Tables S1 and S2).

The differences between the bond lengths of ***cis*-6(*i*Pr)** and ***trans*-6(Cyp)** are summarized in Table 2: the Pt−C bond length is 0.051(4) Å shorter in ***trans*-6(Cyp)**, while the Pt−F distance does not change significantly. The Pt−P distances in ***trans*-6(Cyp)** are equal and lie between the two extreme values observed in ***cis*-6(*i*Pr)**. We have located only four previous structures of Pt(II) fluoride complexes, all of which contain phosphine ligands. Three contain fluoride trans to phosphine: *cis*-$[PtF_2(PPh_3)_2]$ (mean r(Pt−F) = 2.008(2) Å), *cis*-$[Pt(F)\{CH(CF_3)_2\}(PPh_3)_2]$ (r(Pt−F) = 2.03(1) Å), and $[PtF(PEt_3)_3]BF_4$ (r(Pt−F) = 2.043(7) Å).[24−26] The fourth contains a fluoride ligand trans to phenyl, *trans*-$[Pt(F)(Ph)(PPh_3)_2]$ (r(Pt−F) = 2.117(3) Å).[27] It is noteworthy that *cis*-$[PtF\{CH(CF_3)_2\}(PPh_3)_2]$ and $[PtF(PEt_3)_3]BF_4$ show much smaller differences in Pt−P bond lengths compared to ***cis*-6(*i*Pr)**, reiterating the very high trans influence of the unusual {2-$C_5NHF_2(CF_3)$} ligand. The distortions from square-planar geometry of ***cis*-6(*i*Pr)** are comparable to those for *cis*-$[Pt(SiPh_2H)(H)(PCy_3)_2]$ for which the P(1)−Pt−P(2) angle is 113.55(3)°.

The reactions above provide the first evidence for C−F oxidative addition of fluoropyridines by zero-valent platinum. Indeed, the only previous example of intermolecular C−F oxidative addition at platinum involved a phosphine designed to lower barriers by constraining the P−Pt−P bite angle to be much less than 90°.[12] The preference for oxidative addition represents a stark contrast with the chemistry of closely related substrates: pentafluoropyridine reacts with $[Pt(PR_3)_2]$ via a phosphine-assisted pathway to yield *trans*-$[PtR(4\text{-}C_5NF_4)(PR_2F)(PR_3)]$ (reaction with C_6F_6 proceeds similarly but requires a higher temperature),[7,13] while 2,3,5,6-tetrafluoropyridine reacts via C−H bond activation to give *cis*-$[PtH(4\text{-}C_5NF_4)(PR_3)_2]$.[7,28] Thus, we have three quite distinct classes of reaction for a series of closely related substrates: (i) phosphine-assisted C−F bond activation, (ii) C−H oxidative addition, and now (iii) C−F oxidative addition.

The reasons for the switch to oxidative addition are not obvious from a simple consideration of structure. The CF_3 group certainly prevents access to the 4-position of the fluoropyridine, where nucleophilic attack typically occurs.[29] However, there is evidence that the role of the CF_3 group is more complicated and that the strongly electron-withdrawing character of this substituent may be significant, since no analogous reaction is seen with 2,3,5,6-tetrafluoro-4-methylpyridine under the same conditions used above. Solvent polarity may also play a role. Both the C−H oxidative addition with 2,3,5,6-tetrafluoropyridine and the C−F oxidative addition with 2,3,5-trifluoro-4-(trifluoromethyl)pyridine with $[Pt(PR_3)_2]$ (R = *i*Pr, Cy) were performed in hexane, and for $[Pt(PCy_3)_2]$ it was confirmed that C−F oxidative addition also occurs in THF (and at a somewhat faster rate). In contrast, the phosphine-assisted C−F bond activation observed with pentafluoropyridine does require the more polar

(25) Howard, J.; Woodward, P. *J. Chem. Soc., Dalton Trans.* **1973**, 1840.
(26) Russell, D. R.; Mazid, M. A.; Tucker, P. A. *J. Chem. Soc., Dalton Trans.* **1980**, 1737.
(27) Nilsson, P.; Plamper, F.; Wendt, O. F. *Organometallics* **2003**, *22*, 5235.
(28) Solvent effects may also play a role in selectivity, see below.
(29) (a) Brooke, G. M. *J. Fluorine Chem.* **1997**, *86*, 1. (b) Coe, P. L.; Rees, A. J. *J. Fluorine Chem.* **2000**, *101*, 45. (c) Adamson, A. J.; Jondi, W. J.; Tipping, A. E. *J. Fluorine Chem.* **1996**, *76*, 67. (d) Benmansour, H.; Chambers, R. D.; Hoskin, P. R.; Sandford, G. *J. Fluorine Chem.* **2001**, *112*, 133.

THF. The initial product of C−F oxidative addition is *cis*-[Pt(F){2-$C_5NHF_2(CF_3)$}$(PR_3)_2$]], and this is shown to be thermodynamically unstable with respect to *trans*-[Pt(F){2-$C_5NHF_2(CF_3)$}$(PR_3)_2$]. This evidence is consistent with conventional oxidative addition (Pathway 3) and inconsistent with phosphine-assisted C−F oxidative addition (Pathway 2b) which should yield the *trans*-isomer directly.

2.8. Computational Study of the C−F Activation Reaction with 2,3,5-trifluoro-4-(trifluoromethyl)pyridine. In light of the new experimental data obtained with 2,3,5-trifluoro-4-(trifluoromethyl)pyridine, we have returned to computation to assess the impact of altering the substrate on the key stationary points of Pathways 1 and 3. Optimized minima are very similar to those reported above in the pentafluoropyridine study and the computed metal−ligand bonds reproduce the trends in the experimental structures very well (see Supporting Information). The computed relative energies of the three products, ***trans*-3(CF$_3$)** ($E = -10.3$ kcal/mol), ***cis*-4(CF$_3$)** ($E = -18.1$ kcal/mol) and ***trans*-4(CF$_3$)** ($E = -21.8$ kcal/mol) also reproduce the trends seen previously and compare with relative energies of −12.1, −18.8, and −22.9 kcal/mol, respectively, for activation at the 2-position of pentafluoropyridine. Moreover, the *trans*-Pt−fluoride product remains significantly more stable than the *cis*-isomer, consistent with the *cis/trans* isomerization observed experimentally. The key phosphine-assisted C−F activation transition state along Pathway 1 ($E = +24.1$ kcal/mol) and the oxidative addition transition state along Pathway 3 ($E = +22.0$ kcal/mol) also remain very close in energy. This difference of 2.1 kcal/mol is 0.7 kcal/mol greater than that computed for the activation of pentafluoropyridine at the 4-position. This marginal relative stabilization of Pathway 3 is consistent with a shift in favor of oxidative addition for 2,3,5-trifluoro-4-(trifluoromethyl)pyridine, although the change is perhaps too small to be significant. The more secure conclusion is that the delicate balance between these two mechanisms remains.

3. Discussion

3.1. Competing Bond Activation Processes at Pt(0). The accumulated experimental evidence on the reactions of *bis*-trialkylphosphine Pt(0) species with fluoropyridines indicates that three processes are in competition. As discussed here, phosphine-assisted C−F activation at platinum can form Pt(alkyl)(fluorophosphine) complexes, while C−F oxidative addition leads to Pt−fluorides. It has also been shown that C−H oxidative addition may occur if C−H bonds are present on the pyridine.[7] The reactions of [Pt$(PR_3)_2$] species with 2,3,5-trifluoro-4-(trifluoromethyl)pyridine reported here are the first examples of intermolecular C−F oxidative addition at a platinum complex of monodentate phosphines and the first examples of selectivity for C−F over C−H bonds in an intermolecular reaction at Pt.

To date all the computational evidence indicates that Pt−fluorides are the most favored products thermodynamically. This is seen in the greater stability of both isomers of [PtF(4-C_5NF_4)$(PR_3)_2$] over *trans*-[PtR(4-C_5NF_4)$(PR_2F)(PR_3)$] in the present study and in the more exothermic reaction computed for C−F oxidative addition of C_6F_6 to [Pt(dhpe)] compared to the C−H oxidative addition of C_6H_6.[17] Thus C−F oxidative addition invariably yields the most stable products. Moreover, *trans*-[PtF(4-C_5NF_4)$(PR_3)_2$] is energetically more stable than *cis*-[PtF(4-C_5NF_4)$(PR_3)_2$]. When we first reported the formation of the [PtR(Ar^F)$(PR_3)(PR_2F)$] species, we postulated its formation via R/F exchange in *trans*-[PtF(4-C_5NF_4)$(PR_3)_2$].[8] This was based on the precedent of Grushin's F/Ph exchange reaction in [RhF$(PPh_3)_3$];[13] however, this possibility may now be ruled out on the basis of the energetics reported here. A corollary of these results is that C−F bond formation via reductive elimination from 4-coordinate Pt(II) of the type [PtF(R)L_2] will be problematic. This is a significant result given the considerable discussion of this point in the recent literature for related Pd(II) complexes,[30−33] and calculations here show *trans*-[PdF(4-C_5NF_4)$(PH_3)(PH_2Me)$] to be 25.8 kcal/mol more stable than free [Pd$(PH_3)(PH_2Me)$] and pentafluoropyridine.

The different outcomes of C−F bond activation at Pt(0) species are kinetic in origin, and we have shown here that the barriers to phosphine-assisted C−F activation and C−F oxidative addition are very close in energy. Both processes involve concerted mechanisms but with very different transition states. The phosphine-assisted C−F activation involves a 4-center transition state with a relatively large extension of the C−F bond, substantial Pt−fluoropyridyl bond formation and transfer of the released fluoride onto a phosphine that lies cis to the developing M−fluoropyridyl bond. In contrast, in oxidative addition the phosphine ligands are merely spectators, and Pt−fluoride formation involves a 3-center transition state with less C−F elongation and Pt−C bond formation. The difference in transition states indicates that the phosphine-assisted mechanism may overcome some of the electron−electron repulsion between fluorine and metal characteristic of C−F oxidative addition.[17,34]

3.2. Overview of Phosphine-Assisted C−F Bond Activation. Three systems demonstrating formation of M−alkyl/fluorophosphine species from M−phosphine complexes have now been studied in detail by computational methods. Two of these processes involve intermolecular reactions with fluoroaromatics: the reaction of [Pt$(PR_3)_2$] species (R = *i*Pr, Cy) with pentafluoropyridine discussed here and that of [IrMe$(PR_3)_3$] with C_6F_6 described in the preceeding paper.[10] In both cases C−F activation proceeds via very similar transition states that exhibit a metallophosphorane structure. For the iridium system a metallophosphorane intermediate is also located, although this corresponds to a very shallow minimum which reacts further to [Ir(C_6F_5)$(PR_3)_2(PR_2F)$], C_2H_4, and CH_4. Phosphine-assisted C−F bond activation can be described in terms of the nucleophilic attack of an electron-rich metal center on an electron-deficient fluoroaromatic substrate. This process is therefore promoted by more nucleophilic metal centers, and the lower barrier computed for [IrMe$(PH_3)_2(PH_2Me)$] (13 kcal/mol) compared to [Pt$(PH_3)(PH_2Me)$] (25 kcal/mol) is consistent with the lower ionization potential computed for the former (6.4 eV vs 7.4 eV). Phosphine-assisted C−F bond activation proceeds without a dienyl intermediate characteristic of the classical Meisenheimer mechanism but is instead characterized by a single, very late transition state in which the M−fluoropyridyl bond is almost fully formed. The strength of this bond therefore determines the selectivity of reaction; in particular, we have shown for iridium that the activation barrier decreases in size

(30) (a) Grushin, V. V. *Chem. Eur. J.* **2002**, *8*, 1006. (b) Grushin, V. V. *Organometallics* **2000**, *19*, 1888.
(31) Yandulov, D. V.; Tran, N. T. *J. Am. Chem. Soc.* **2007**, *129*, 1342.
(32) Grushin, V. V.; Marshall, W. J. *Organometallics* **2007**, *26*, 4997.
(33) Hull, K. L.; Anani, W. Q.; Sanford, M. S. *J. Am. Chem. Soc.* **2006**, *128*, 7134.
(34) Bosque, R.; Clot, E.; Fantacci, S.; Maseras, F.; Eisenstein, O.; Perutz, R. N.; Renkema, K. B.; Caulton, K. G. *J. Am. Chem. Soc.* **1998**, *120*, 12634.

as the number of ortho-fluorine substituents increases. For both Pt- and Ir-M(alkyl)(fluorophosphine) species are significantly less stable than the M(fluoride)(phosphine) alternatives, indicating the bond strength relationship: $D_{M-F} + D_{P-R} > D_{M-R} + D_{P-F}$.

The third example of M(alkyl)(fluorophosphine) formation is the reversible isomerization of [RhF(PPh_3)$_3$] to *trans*-[RhPh(PPh_3)$_2$($PFPh_2$)], and this differs from the above cases in that it is an intramolecular process.[13] The mechanism involves F transfer to produce a shallow metallophosphorane intermediate, followed by Ph transfer to Rh. The reversibility of the reaction and the small energy difference between reactants and products imply the bond energy relation: $D_{Rh-F} + D_{P-Ph} \approx D_{Rh-Ph} + D_{P-F}$. This differs from the relationship established for platinum and iridium above and may reflect the fact that M−alkyl bonds are generally weaker than M−aryl bonds. So far R/F isomerization has only been observed in the rhodium system, and this may reflect the less electron-rich character of the PPh_3 ligand in this case, which makes it more prone to *intramolecular* nucleophilic attack by the neighboring fluoride. For the platinum and iridium systems featuring more electron-rich trialkylphosphines the calculations predict that, although R/F isomerization is thermodynamically favored, exchange via metallophosphorane species may suffer from high barriers (cf. Figure 3 above and Figure 3 in the preceding paper[10]). Thus, for *trans*-[PtR(4-C_5NF_4)(PR_2F)(PR_3)] R/F exchange (R = *i*Pr, Cy) has yet to be observed experimentally. Instead these electron-donating phosphines confer sufficient nucleophilicity upon the metal center to induce the phosphine-assisted *intermolecular* C−F activation. As shown in the preceding paper[10] (and predicted previously[13]), the transferring fluoride becomes so highly nucleophilic in the transition state of this process that it can attack even a relatively electron-rich phosphorus center. In this context, it appears that the two distinct types of chemistry involving metallophosphorane species (C−F bond activation and isomerization) may be mutually exclusive.[13]

4. Conclusions

We have used both computational and experimental methods to rationalize the diverse reactivity of [Pt(PR_3)$_2$] species toward fluoropyridines. The calculations have shown that a novel phosphine-assisted C−F activation mechanism is possible with these electron-rich precursors. The barrier associated with this process is, however, very similar to that for conventional oxidative addition and we have shown experimentally that the balance between these processes is extremely delicate. Our experiments provide the first examples of conventional oxidative addition of aromatic C−F bonds at Pt(0) species with monodentate phosphines.

Phosphine-assisted C−F activation is emerging as a novel mechanism for C−F bond activation where an electron-rich organometallic attacks an electron-deficient substrate with transfer of the released fluoride onto a phosphine that lies cis to the developing M−C bond. The phosphine-assisted pathway has general implications for the reactivity of metal phosphine complexes toward attack by fluorocarbons in C−F activation processes. We have noted that it can provide routes to metal alkyls with fluorophosphine ligands or even to metal fluoride complexes. Low-valent MF(PR_3) species are often quite stable thermodynamically and are therefore not prone to reductive elimination or conversion to metal fluorophosphine alkyls. However, the reversible isomerization of [RhF(PPh_3)$_3$] signals that a change to aryl substituents can reduce the stability of the fluoride complexes markedly.

5. Experimental Section

5.1. General procedures. All operations were performed under an argon atmosphere, either on a high-vacuum line (10^{-4} mbar) using modified Schlenk techniques, on standard Schlenk (10^{-2} mbar) lines or in a glovebox. Solvents for general use (hexane, benzene, toluene) were of AR grade, dried by distillation over standard reagents, or with a solvent purification system, and stored under Ar in ampoules fitted with Young's PTFE stopcocks. Deuterated solvents were dried by stirring over potassium, and were distilled under high vacuum into small ampoules with potassium mirrors.

Photochemical reactions, at room temperature, were performed in glass NMR tubes fitted with Young's PTFE stopcocks, using a Philips 125 W medium-pressure mercury vapor lamp with a water filter (5 cm).

All NMR spectra were recorded on Bruker AMX500 spectrometers in the same type of tube. All ^{1}H NMR spectra were recorded at 500.2 MHz; chemical shifts are reported in ppm (δ) relative to tetramethylsilane and are referenced using the chemical shifts of residual protio solvent resonances (benzene, δ 7.16). The ^{31}P{^{1}H} NMR spectra were recorded at 202.5 MHz and are referenced to external H_3PO_4. ^{19}F NMR spectra were recorded at 470.5 MHz and referenced to external $CFCl_3$ at δ 0 or internal C_6F_6 at δ −162.9.

Mass spectra were recorded by the University of York analytical services either on a VG Auto-Spec mass spectrometer in FAB mode, or on a Waters GCT instrument fitted with a Linden LIFDI probe. The value of *m*/*z* is listed for ^{194}Pt unless otherwise stated. Infrared spectra were recorded as KBr disks (prepared in the glovebox) on a Mattson research series FTIR spectrometer fitted with a KBr beam splitter. The sample chamber was purged with dry, CO_2-free air.

Chemicals were obtained from the following sources: potassium tetrachloroplatinate from Aldrich (or recovered from platinum residues by a standard procedure); P*i*Pr$_3$, PCy_3, and $PCyp_3$ from Strem, 2,3,5-trifluoro-4-trifluoromethylpyridine from Fluorochem.

5.2. Synthesis of [Pt(PR_3)$_2$]. *trans*-[$PtCl_2$(PR_3)$_2$] (1 g) was placed in a 50 mL Schlenk flask containing PR_3 (0.13 g) and a magnetic stirring bar and suspended in THF (2 mL). A 0.33 mol dm^{-3} THF solution of sodium naphthalenide, freshly prepared from freshly cut sodium (0.5 g) and naphthalene (2.2 g in 50 mL of THF), was added dropwise to the suspension. The addition was halted at the point when the dark green color of the naphthalenide persisted. After 2 h stirring the solvent was removed under vacuum and the excess naphthalene removed by sublimation (10^{-4} mbar).[35] The dark-brown solid residue was extracted with hexane in the glovebox and the extract transferred into a funnel and filtered through paper to yield a yellow solution of [Pt(PR_3)$_2$]. This solution was either employed directly in the next step or pumped to dryness before use. The following accounts describe synthesis using solid *trans*-[$PtCl_2$(PR_3)$_2$].

5.3. Synthesis of *cis*-[Pt(F){2-$C_5NHF_2(CF_3)$}(P*i*Pr$_3$)$_2$], *cis*-6(*i*Pr). [Pt(P*i*Pr$_3$)$_2$] (0.4 g, 0.78 mmol) was dissolved in hexane (~5 mL) in the glovebox, and 2,3,5-trifluoro-4-trifluoromethylpyridine (0.3 g, 1.5 mmol) was added. The solution was left in the glovebox at room temperature for 2 days; colorless crystals of ***cis*-6(*i*Pr)** formed. The solvent was decanted off, and the crystals were dried in vacuo. Yield 0.32 g, 0.45 mmol (58%). If the solution was left for a further week and the hexane was allowed to reduce in volume by evaporation, the yield could be increased to 82%. IR, KBr disk, cm^{-1}: 2983 (s), 2964 (m), 2918 (s sh), 1568 m, 1543 (w), 1517 (w), 1472 (s, sh), 1461 (s), 1370 (s), 1332 (s, b), 1258 (m), 1167(s), 1089 (w), 1070 (w),1010 (m), 1002 (w), 910 (w),

(35) (a) Yoshida, T.; Otsaka, S. *Inorg. Synth.* **1979**, *19*, 105. (b) Immirzi, A.; Musco, A. *Inorg. Chim. Acta* **1975**, *12*, L23.

892 (m), 801 (w), 773 (w), 717 (w), 669 (s), 653 (w), 599 (m sh), 552 (s), 533 (m), 486 (m) and 447 (m).

Mass spectrometry, LIFDI$^+$ (*m*/*z*): $C_{24}H_{43}F_6NP_2Pt$ 715.3 (M^+) 100%.

Anal. calcd for $C_{24}H_{43}F_6NP_2Pt$: C, 40.22; H, 6.05; N, 1.95. Found: C, 40.35; H, 6.45; N, 1.70.

5.4. Synthesis of *trans*-[Pt(F){2-$C_5NHF_2(CF_3)$}($PCyp_3$)$_2$], *trans*-6(Cyp). [Pt($PCyp_3$)$_2$], (0.2 g, 0.30 mmol) was dissolved in hexane (~5 mL) in the glovebox, and 2,3,5-trifluoro-4-trifluoromethylpyridine (0.11 g, 0.55 mmol) was added. The solution was left in the glovebox at room temperature for 2 weeks. Colorless crystals of ***trans*-6(Cyp)** formed. The solvent was decanted off, and the product was dried under vacuum. Residual naphthalene was removed by sublimation at room temperature. Yield 0.22 g, 0.25 mmol (83%).

IR, KBr disk, cm^{-1}: 2964 (s), 2864 (s), 1486 (w), 1448 (m), 1320(w), 1300 (m), 1259 (m), 1232 (w), 1223 (vw), 1116 (s), 1107 (s), 1069 (m), 1053 (m), 1030 (m), 943 (w), 902 (m), 805 (w), 702 (vw), 596 (b w), 531 (m sh), 523 (s b), 510 (m, sh), 491 (w), 478 (m sh), 458 (w) and 444 (w).

Mass spectrometry, FAB$^+$ (*m*/*z*): $C_{36}H_{55}F_6NP_2Pt$ 872.3 ($M + H)^+$ 7%, 871.3 (M^+) 7%, 852.3 ($M^+ - F$) 100%, 669.3 [Pt($PCyp_3$)$_2$ $- H]^+$ 10%.

5.5. Synthesis of *trans*-[Pt(F){2-$C_5NHF_2(CF_3)$}(PCy_3)$_2$], *trans*-6(Cy). [Pt(PCy_3)$_2$] (0.2 g, 0.26 mmol) was dissolved in hexane (~5 mL) in the glovebox, and 2,3,5-trifluoro-4-trifluoromethylpyridine (0.10 g, 0.50 mmol) was added. The solution was left in the glovebox at room temperature for 2 weeks. Colorless crystals of ***trans*-6(Cy)** formed. The solvent was decanted off, and the product was dried under vacuum. Residual naphthalene was removed by sublimation at room temperature. Yield 0.15 g, 0.16 mmol (59%). Another experiment was left for 3 weeks and yield was 0.175 g (69%).

IR, KBr disk, cm^{-1}: 2931 (s), 2870 (s), 1575 (m), 1559 (w sh), 1490 (s), 1356 (s), 1335 (m), 1319 (s), 1275 (m), 1250 (w), 1155 (s), 1094 (m), 1019 (m), 1017 (m), 785 (w), 738 (m), 733 (m sh), 711 (m), 670 (vw), 660 (w), 651 (w sh), 576 (m), 562 (w), 545 (w), 537 (m), 517 (m), 490 (w), 464 (m), 455 (w) and 442 (vw).

Mass spectrometry: LIFDI$^+$, (*m*/*z*): $C_{42}H_{67}F_6NP_2Pt$ 955.4 (M^+) 50%.

Anal. calcd for $C_{42}H_{67}F_6NP_2Pt$: C, 52.71; H, 7.06; N, 1.46. Found: C, 51.8; H, 7.9; N, 1.5.

5.6. Monitoring of Reactions by NMR. The reactions of Pt(PR_3)$_2$ with 2,3,5-trifluoro-4-trifluoromethylpyridine in benzene-d_6 were monitored in situ in an NMR tube by ^{19}F and ^{31}P NMR spectroscopy.

R = *i*Pr. The reaction was monitored daily for the first few days. The major product was ***cis*-6(*i*Pr)** with traces of ***trans*-6(*i*Pr)**. The reaction was complete after 2 days, yielding the *cis*-isomer with traces of the *trans*-isomer. Provided that the solution was kept in the dark, this solution was stable for at least 1 month (monitoring every 2 days approx.). There was no trace of platinum(alkyl)-(fluorophosphine) products at any stage, nor any other platinum fluoride complexes.

R = Cyp or Cy. The reaction was monitored in the NMR tube every 2 days. Both *cis* and *trans* products were observed after 2 days. The reaction was complete after about 2 weeks. At this stage ***trans*-6(Cyp)** and ***trans*-6(Cy)**, respectively, were the only products. There was no trace of platinum(alkyl)(fluorophosphine) products at any stage, nor any other platinum fluoride complexes.

5.7. X-ray Cystallography. Diffraction data were collected on a Bruker Smart Apex diffractometer with Mo Kα radiation (λ = 0.710 73 Å) using a SMART CCD camera. Diffractometer control, data collection, and initial unit cell determination were performed using "SMART" (v5.625 Bruker-AXS). Frame integration and unit-cell refinement were carried out with "SAINT+" (v6.22, Bruker AXS). Absorption corrections were applied using SADABS (v2.03, Sheldrick). The structure was solved by direct methods using SHELXS-97 (Sheldrick, 1997) and refined by full-matrix least-squares methods using SHELXL-97 (Sheldrick, 1997).[36] Hydrogen atoms were placed using a "riding model" and were included in the refinement at calculated positions. For ***cis*-6(*i*Pr)**, disorder of the CF_3 group was modeled as two positions differing by a 60° rotation. Their occupancies were optimized as ~85% a form and 15% b form. The C−F bond lengths of the CF_3 group were restrained to be the same, and the spacings between the fluorine atoms were also restrained to be the same. The anisotropic displacement parameters of "opposite" fluorine atoms were constrained to be the same. For ***trans*-6(Cyp)**, there was evidence of disorder in some of the cyclopentyl rings. However, attempts to model this using a two-site model failed, probably because the two sites are too close to separate. This disorder leads to an apparent shortening of some of the C−C bond lengths. Crystallographic data are given in Table 3. Details for ***trans*-6(Cy)** are provided in the Supporting Information.

Table 3. Crystal and Structure Refinement Data

complex	***cis*-6(*i*Pr)**	***trans*-6(Cyp)**
empirical formula	$C_{24}H_{43}F_6N_1P_2Pt_1$	$C_{36}H_{55}F_6N_1P_2Pt_1$
formula weight	716.62	872.84
temperature (K)	115(2)	110(2)
crystal system	monoclinic	monoclinic
space group	$P2_1/n$	$P2_1/c$
unit cell dimensions		
a (Å)	15.9928(11)	10.5548(6)
b (Å)	10.8838(8)	19.6695(10)
c (Å)	16.4567(11)	17.3098(9).
β (deg)	100.3800(10)	100.8160(10)
V (Å^3)	2817.6(3)	3529.8(3)
Z	4	4
density (calcd, Mg/m^3)	1.689	1.642
absorption coeff (mm^{-1})	5.146	4.125
F(000)	1424	1760
crystal size(mm^3)	0.22 × 0.16 × 0.03	0.27 × 0.14 × 0.06
θ range (deg)	1.63 to 28.32	1.58 to 30.00.
reflections collected	28466	38910
independent reflections	7007 [R(int) = 0.0319]	10154 [R(int) = 0.0307]
data/restraints/params	7007/21/329	10154/0/416
goodness-of-fit on F^2	1.034	1.035
final R indices [$I > 2\sigma(I)$]	R1 = 0.0272, wR2 = 0.0610	R1 = 0.0285, wR2 = 0.0673
R indices (all data)	R1 = 0.0374, wR2 = 0.0644	R1 = 0.0374, wR2 = 0.0711
CCDC number	684870	684871

5.8. Computational Methods. All density functional theory (DFT) calculations described in this paper were performed using the Gaussian03[37] package and employed the BP86[38] functional. SDD pseudopotentials and the associated basis sets were used to describe Pt,[39] while 6-31G(d,p) basis sets were used for all other atoms.[40] Geometry optimizations were performed without symmetry constraints, and stationary points were characterized as minima or transition states by vibrational analysis. Transition states were further characterized by IRC calculations and subsequent geometry optimizations to confirm the nature of the minima involved in each step. All energies include a correction for zero-point energy.

(36) Sheldrick, G. M. *SHELXS-97, Program for Structure Solution*; University of Göttingen: Göttingen, Germany, 1997. Sheldrick, G. M. *SHELXL-97: Program for the Refinement of Crystal Structures*; University of Göttingen: Göttingen, Germany, 1997.

(37) Frisch, M. J.; et al. *Gaussian 03, Revision C.02*; Gaussian, Inc.: Wallingford CT, 2004.

(38) (a) Becke, A. D. *Phys. Rev. A* **1988**, *38*, 3098. (b) Becke, A. D. *J. Chem. Phys.* **1993**, *98*, 1372. (c) Becke, A. D. *J. Chem. Phys.* **1993**, *98*, 5648. (d) Vosko, S. H.; Wilk, L.; Nusair, M. *Can. J. Phys.* **1980**, *58*, 1200. (e) Becke, A. D. *J. Chem. Phys.* **1986**, *84*, 4524. (f) Perdew, J. P. *Phys. Rev. B* **1986**, *33*, 8822.

(39) Andrae, D.; Häusserman, U.; Dolg, M.; Stoll, H.; Preuss, H. *Theor. Chim. Acta* **1990**, *77*, 123.

(40) (a) Hehre, W. J.; Ditchfield, R.; Pople, J. A. *J. Chem. Phys.* **1972**, *56*, 2257. (b) Hariharan, P. C.; Pople, J. A. *Theor. Chim. Acta* **1973**, *28*, 213.

Acknowledgment. A.N.'s stay at the University of York was funded by the Ministerio de Ciencia y Tecnología of Spain (Project BQU2002-04110-C02-02). The support of the EPSRC for a postdoctoral fellowship (S.E.) through Grant GR/T28539/01 is gratefully acknowledged.

Supporting Information Available: ^{1}H, ^{19}F, and ^{31}P NMR spectra of ***cis*-6(*i*Pr)** and ***trans*-6(*i*Pr)**. X-ray crystal structure for ***trans*-6(Cy)**, Cartesian coordinates for all the structures calculated, and complete list of authors for ref 37, X-ray crystallographic files for ***cis*-6(*i*Pr)**, ***trans*-6(Cyp)**, and ***trans*-6(Cy)** (CIF). This material is available free of charge via the Internet at http://pubs.acs.org.

JA8046238